.

Citation: *Egypt.Acad.J.Biolog.Sci. (C.Physiology and Molecular biology) Vol. 15(2) pp471-485 (2023)*
DOI: 10.21608/EAJBSC.2023.321788

Egypt. Acad. J. Biolog. Sci., 15(2):471-485 (2023)

Egyptian Academic Journal of Biological Sciences
C. Physiology & Molecular Biology
ISSN 2090-0767
www.eajbsc.journals.ekb.eg

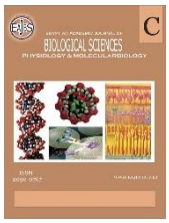

Biochar and Biochar Magnetite of *Spirulina platensis* to Remove Cadmium Ions from Aqueous Solutions

Khitam J. Mushtaq and Sadiq K. L. Alzurfi*
Department of Ecology and Pollution - Faculty of Science - University of Kufa-Iraq
***E-mail: sadiqk.alzurfi@uokufa.edu.iq**

ARTICLE INFO
Article History
Received:10/9/2023
Accepted:17/10/2023
Available:21/10/2023

Keywords:
Biochar, H_2O_2, MBC, FESEM, Spirulina.

ABSTRACT

An investigation was conducted using both biochar and magnetic biochar. Have been utilized as an effective, affordable, secure, and ecologically friendly way to get rid of heavy metals like cadmium. Microalgae from Spirulina platensis were used to make biochar by burning it. We mix biochar with hydrogen peroxide to create functional groups on the surface by using ice bath sonication which is biochar activate (BC). Also, magnetic biochar (MBC) has been prepared by mixing biochar activated with Fe_3O_4 (2:1 mole ratio) respectively. Two concentrations of aqueous solutions (5 ppm and 10 ppm) were mixed with two weights of biochar and magnetic biochar (0.1 and 0.5 g) for 10, 20, and 40 minutes. The concentration of cadmium (5 ppm) with 0.5 g of biochar (BC) after 40 minutes removed 97.58% of cadmium ion from the aqueous solution. On the other hand, magnetic biochar (MBC) (0.5 g) with 5 ppm of cadmium solution after 40 minutes could remove 100% of cadmium ions. We character BC, MBC, and biochar treated with cadmium ions by using FTIR, FESEM, EDX, and XRD studies. These analytical results indicate that the effective groups in biochar and magnetic biochar can adsorb heavy metals by carboxyl, hydroxyl, and carbonyl groups. The findings of the investigation on magnetic biochar revealed that, in addition to carbonyl, hydroxyl, and carboxylic groups, the substance also included magnetite. The findings made it very clear that removing cadmium with biochar reduced their risk and did it in a quick, inexpensive, and environmentally beneficial manner.

INTRODUCTION

Heavy metal contamination in drinking water and wastewater poses a major threat to the environment and all living things on land, in the air, and in the water. Heavy metals were processed using a variety of cutting-edge biological and conventional techniques based on nanomaterials. Microalgae are a significant class of microorganisms used in biological processes that can remove heavy metals from wastewater and have numerous environmental uses (Priatni *et al.,* 2018). One of the potential biological treatment methods is the use of microalgae to remove heavy metals from contaminated soil or water (Goswami *et al*.,2022). Polysaccharides, proteins, and lipids found on the surface of microalgae have a variety of functional groups, such as carboxyl, hydroxyl, carbonyl, and phosphodiester groups, that help heavy metal ions bind well (Pragya *et al.,* 2013). Algae are photosynthetic creatures that may live in freshwater, seawater, or sewage. In recent years, microalgae have been used to extract dangerous metals from wastewater treatment plants and transform them into less toxic molecules (Goh *et al.*,2022). Blue-green Spirulina platensis is a multicellular prokaryote (alga).

In order to bind heavy metals, its cell wall mostly consists of carbohydrates (cellulose and alginate) and organic lipids, which include a variety of functional groups (such as amino and carboxyl, hydroxyl, imidazole, phosphate, sulfonate, thiol, etc.) (Priatni *et al.*, 2018). The stable carbon content of biochar is high, and it also has several nutrients. Because of its architecture with numerous micropores and resulting large surface areas, as well as its numerous functional groups, it is widely employed in carbon sequestration and soil improvement. Heavy metals in the soil and water can be removed using biochar as an adsorbent and residue (Qiu *et al.*, 2022). The present study aims to determine the role of microalgae in the biological treatment of heavy metals, the mechanism of absorption of heavy metals, and the factors affecting the efficiency of removal.

MATERIALS AND METHODS

Spirulina platensis came from the Star West Company in China. It was sieved and processed to make biochar. Other chemicals were purchased from Sigma-Aldrich (M) Sdn Bhd, including ethanol, sodium hydroxide, hydrochloric acid, cadmium sulfate, ferrous sulfate, and ferric chloride. The chemicals were used directly after receipt without any additional processing.

The two procedures that made up the assembly process for the composite magnetic biochar-based adsorbent (Scheme 1) were the production of MBC and biochar. Raw Spirulina platensis was first pyrolysis to create biochar utilizing a number of different input factors, including the pyrolysis temperature, heating time, and impregnation ratio (raw Spirulina platensis/H_2O_2). The obtained biochar was then combined with magnet materials to generate composite magnetic biochar. The biochar and magnetic biochar were used for the Cd^{2+} adsorption process after being analyzed.

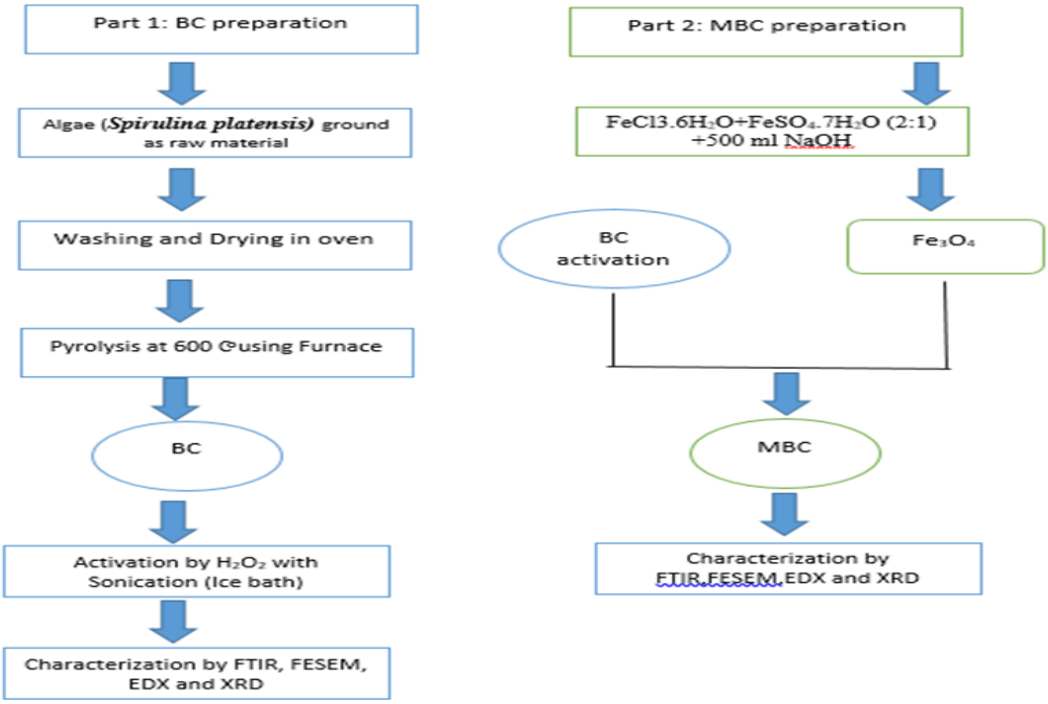

Scheme 1: A summary diagram showing the preparation and testing of the composite magnetic biochar.

Biochar Preparation:

The Spirulina platensis was continuously cleaned with distilled water to remove pollutants and dust from its surface and then dried for 24 hours at 105°C. The mesh size was decreased to the required 0.5

mm by passing the dried material through the proper sieves (Vibratory Sieve Shaker AS 200 Digit cA Model). It was then stored in an airtight container at room temperature until it was needed. Spirulina platensis was utilized to make charcoal by slow pyrolysis. We updated the preparation parameters in accordance with those that had been preoptimized in a tube furnace at a pyrolysis temperature of 600 °C, a reaction time of 4 hours (Kim *et al.,* 2019)..

Biochar Activation:

The next step is to create function groups on the surface of biochar by using hydrogen peroxide which is an alternative to the sodium hydroxide method (Kim et al., 2019). To prepare biochar to activate (BC activate), we disperse 1g of biochar in 20 mL of hydrogen peroxide (H_2O_2, 35%) then use bath sonication as the source of energy to create the hydroxyl, carboxyl and carbonyl groups. The temperature during the experiment must be between 10-25ºC for 1h after that filtration, and the biochar activated on filter paper overnight to dry and washed with acetone three times.

Magnetic Preparation:

Magnetic iron oxide was created using the co-precipitation approach (Al-Kazazz et al., 2016). Fe_3O_4 MNPs are as follows: magnetic biochar was made using Fe_3O_4 nanoparticles. The magnetic nanoparticles were precipitated using methods that used ferrous sulfate ($FeSO_4$) and ferric chloride ($FeCl_3.6H_2O$) in a 2:1 ratio.

Preparation of Modified (magnetic) Biochar:

Following the production of MBC, biochar was added to 750 mL of deionized water by adding 5 g of Fe_3O_4 and 10 g of BC over a period of two hours. The magnetic biochar is dried for 24 hours at a temperature of 45 °C after being repeatedly washed with ethanol and then distilled water (Baltrėnaitė *et al.,* 2017).

Adsorption Study:

A 1000 ppm Cd^{2+} stock solution was prepared by dissolving 1.8 g of cadmium sulfate in deionized water. The stock solution was then diluted to different concentrations (5 and 10 ppm) for batch studies. The solution underwent a number of modifications to obtain the best adsorption performance. Batch adsorption studies were performed by adding biochar to a cadmium-aqueous solution in an Erlenmeyer flask. The adsorbent was used in doses of 0.1 and 0.5 g for a total of 10, 20, and 40 minutes.

$$R\% = \frac{(Ci - Cf)}{Ci} \times 100 \quad \ldots\ldots\ldots\ldots\ldots\ldots\ldots\ldots (1)$$

Sorption capacity of biochar was calculated according to the following formula:

$$A = \frac{C1 - Cf}{m} \times v\ (mg.g^{-1}) \ldots\ldots\ldots\ldots\ldots\ldots\ldots (2)$$

Statically Analysis:

All data were analyzed using a univariate ANOVA. The probability threshold of 5% (P 0.05) was selected to illustrate the statistical difference. SPSS 26.0 (IBM, Chicago, IL, USA) is being used.

RESULTS AND DISCUSSION

At a concentration of 5 ppm, the highest rate of cadmium removal from water treated with biochar was found at a dose of (0.5) gm of biochar for (40) minutes. The lowest rate of cadmium removal was found at a dose of (0.1) gm of biochar for (10) minutes (Fig. 1). The statistical analysis's findings revealed that there were notable variations between weights and times (Table 1). The lowest removal rate was 55.09% at (10) minutes and a dose of (0.1) grams of biochar. The highest removal rate was 96.73% for cadmium at a concentration of 10 ppm in water treated with biochar at a dose of (0.5) gm and a time of (40) minutes (Fig. 2). The statistical analysis's findings revealed that there were no appreciable variations between weights and times (Table 2).

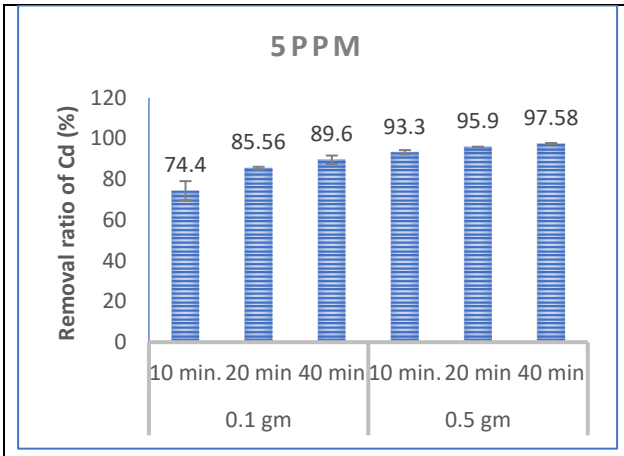

Fig.1: Removal ratio of cadmium (5 ppm) by biochar activate.

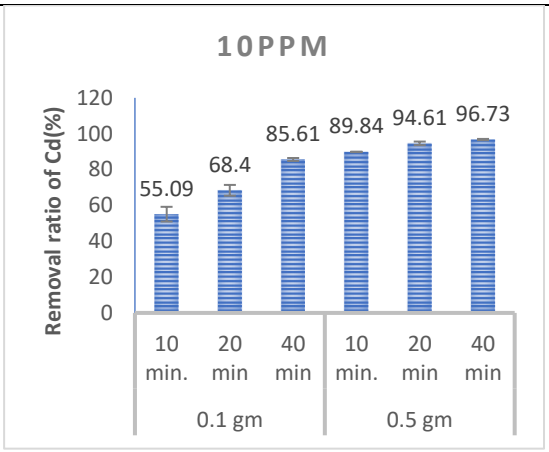

Fig.2: Removal ratio of cadmium ions (10 ppm) by biochar activate.

Table 1: Variance analysis test of cadmium (5 ppm) treated by biochar

Tests of Between-Subjects Effects Dependent Variable: Cadmium						
Source	**Type III Sum of Squares**	**Df**	**Mean Square**	**F**	**Sig.**	**Partial Eta Squared**
Corrected Model	1092.557[a]	5	218.511	46.073	.000	.950
Intercept	143837.449	1	143837.449	30327.965	.000	1.000
Dose	692.168	1	692.168	145.943	.000	.924
Time	301.214	2	150.607	31.755	.000	.841
Dose * Time	99.175	2	49.587	10.455	.002	.635
Error	56.913	12	4.743			
Total	144986.919	18				
Corrected Total	1149.470	17				
a. R Squared = .950 (Adjusted R Squared = .930)						

Table 2: Variance analysis test of cadmium (10 ppm) treated by biochar

Tests of Between-Subjects Effects Dependent Variable: Cadmium						
Source	**Type III Sum of Squares**	**Df**	**Mean Square**	**F**	**Sig.**	**Partial Eta Squared**
Corrected Model	4076.898[a]	5	815.380	175.848	.000	.987
Intercept	120195.411	1	120195.411	25921.750	.000	1.000
Dose	2597.523	1	2597.523	560.191	.000	.979
Time	1049.652	2	524.826	113.186	.000	.950
Dose * Time	429.723	2	214.861	46.338	.000	.885
Error	55.642	12	4.637			
Total	124327.951	18				
Corrected Total	4132.540	17				
a. R Squared = .987 (Adjusted R Squared = .981)						

The lowest percentage of cadmium removal was (97.6%) at a dose of (0.1) gm of MBC and a time of (10) minutes. At a concentration of 5 ppm in water treated with MBC, the highest percentage of cadmium removal was (100%) at a dose of (0.5) gm of MBC and a time of (40) minutes (Fig. 3). The statistical analysis findings revealed that there were appreciable variations in weights and timings (Table 3). The lowest removal rate

was 90.36 percent at 10 minutes and 0.1 grams of MBC, and the highest removal rate was 99.96 percent for 10 ppm of cadmium in water treated with 0.5 grams of MBC and 40 minutes (Fig. 4). There were no appreciable variations between weights and times, according to the statistical analysis findings (Table 4).

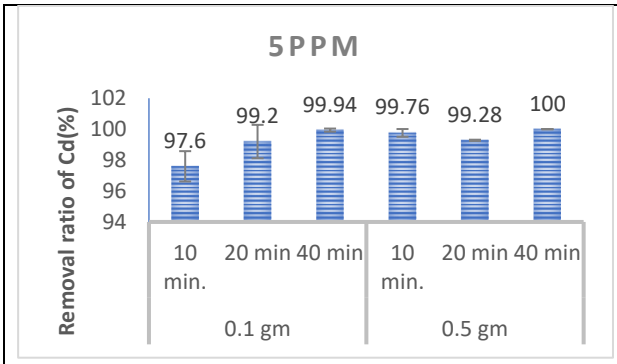

Fig.3: Removal ratio of cadmium (5 ppm) by MBC.

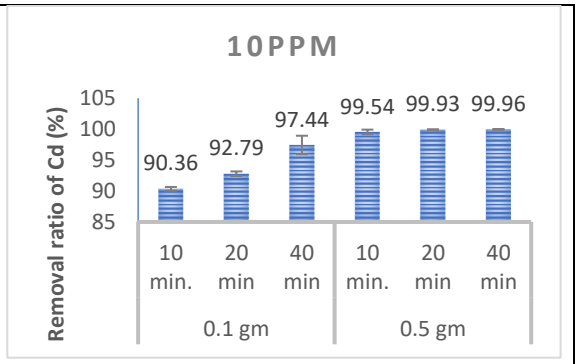

Fig.4: Removal ratio of cadmium (10 ppm) by MBC.

Table 3: Variance analysis test of cadmium (5 ppm) treated by magnetic biochar(MBC).

Tests of Between-Subjects Effects Dependent Variable: Cadmium						
Source	**Type III Sum of Squares**	**Df**	**Mean Square**	**F**	**Sig.**	**Partial Eta Squared**
Corrected Model	12.039[a]	5	2.408	6.540	.004	.732
Intercept	177500.736	1	177500.736	482164.260	.000	1.000
Dose	2.614	1	2.614	7.102	.021	.372
Time	4.986	2	2.493	6.772	.011	.530
Dose * Time	4.438	2	2.219	6.028	.015	.501
Error	4.418	12	.368			
Total	177517.192	18				
Corrected Total	16.456	17				
a. R Squared = .732 (Adjusted R Squared = .620)						

Table 4: Variance analysis test of cadmium (10 ppm) treated by magnetic biochar(MBC).

Tests of Between-Subjects Effects Dependent Variable: Cadmium						
Source	**Type III Sum of Squares**	**Df**	**Mean Square**	**F**	**Sig.**	**Partial Eta Squared**
Corrected Model	255.375[a]	5	51.075	113.955	.000	.979
Intercept	168219.334	1	168219.334	375317.378	.000	1.000
Dose	177.473	1	177.473	395.963	.000	.971
Time	43.018	2	21.509	47.989	.000	.889
Dose * Time	34.885	2	17.442	38.916	.000	.866
Error	5.378	12	.448			
Total	168480.088	18				
Corrected Total	260.754	17				
a. R Squared = .979 (Adjusted R Squared = .971)						

The results of employing biochar to remove cadmium-contaminated aqueous solutions corroborated our findings by showing that biochar has the capacity to adsorb cadmium from aqueous solutions. (Yusuff et al., 2022; Jasim and Alzufri, 2022). The results showed a gradual increase in the removal ratio of cadmium at concentrations of 5 ppm and 10 ppm treated by biochar at a dose of 0.1 gm and 0.5 gm within 40 minutes at a constant temperature of 25–30 degrees Celsius. Due to the absorbent material's available surface area and the presence of active groups that aid in binding cadmium ions to it (Lei et al., 2019). While agglomeration of the micro-components of the absorbents, which reduces the distance between the micro-components of the absorbent materials and prevents the increase in efficiency, occurs at the lowest adsorption rate of cadmium at concentrations of 5 ppm and 10 ppm of cadmium ions when weighing (0.1) g of activated biochar at a time of (10) minutes (Kadhum and Albayati, 2022). It was also discovered that cadmium adsorption rates were higher with an increase in the adsorption dose of magnetic biochar compared to its predecessor biochar, where rapid uptake is related to the availability of active sites on the surface. These positive results and differences in adsorption efficiency were obtained and noted after adding Fe_3O_4 prepared in the laboratory to biochar to remove cadmium ions from the aqueous solution (Hassan et al., 2022), in addition to the primary removal mechanism, which is mostly accomplished by interactions with functional groups, electrostatic adsorption, and ion exchange between heavy metals and adsorbents (Luo et al., 2018). Figures 3 and 4 show that when we add magnetism to the biochar, the removal rates go up and the results are much better. This is because the sorbent material has a bigger surface area, its absorbing surface is better, and there are more places for the active grates to go. The highest removal ratio of cadmium was recorded, and its concentration after treatment was 10 ppm (Wang et al., 2018). Finally, it was found that the adsorption process, whether for biochar or magnetic biochar for cadmium, decreases when the concentrations and weights used for treatment are increased. This is because the cadmium ion competes with the small area of the components of biochar and magnetic biochar for binding sites on the surface of the adsorbent material. While the lower concentration offers a driving force sufficient to overcome all resistances imparted to the solutes between the solid (biochar) and liquid (aqueous solution) phases, the adsorption resistance (Cd) lowers as the driving force for mass transfer increases (Aniagor et al., 2021).

FESEM and EDX Spectra Analysis:

The biochar was examined after activation resulting from algae, and it was found that it is composed of basic elements such as carbon and oxygen, as shown by the FESEM image that appears in Figure (5). While Figure 6 shows a FESEM of the compound magnetic biochar, it also shows a picture of the elements from which the compound is composed: carbon, iron, and oxygen. Figure 7 is a field emission scanning electron microscopy (FESEM) analysis of the activated biochar (0.1 g) after treatment with cadmium ions (10 ppm) at a time contact of 40 min. The FESEM images show the morphology of the biochar surface after the activation process. On the other hand, FESEM images show the morphology of magnetic biochar (MBC) (0.1 g) after treatment with cadmium ions (10 ppm) at a time contact of 40 min (Fig. 8). Also, FESEM images could measure the nanoparticle size of the magnetic (Fe_3O_4), which is around 36±6. In addition, how these sit and homogenize distribution on the surface of biochar Moreover, we used Energy Dispersive X-ray analysis (EDX) as another technique to improve the composite structure of the BC and MBC.

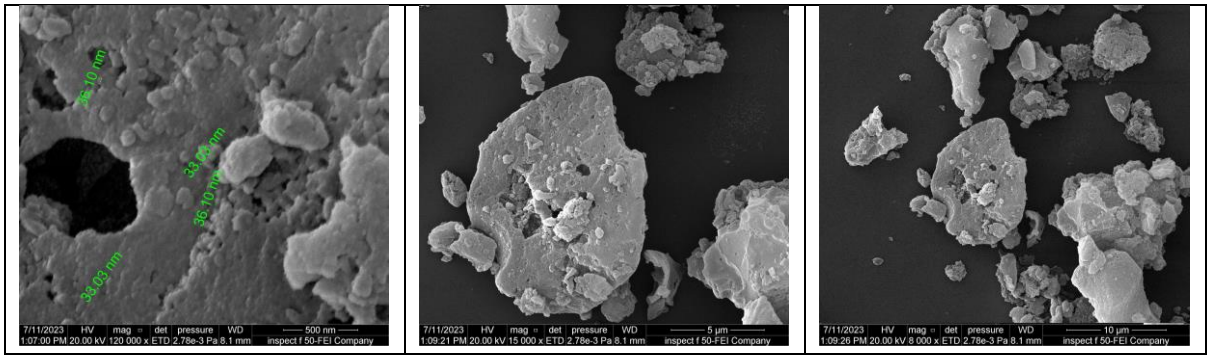

Fig.5: FESEM of biochar activation before treatment**.**

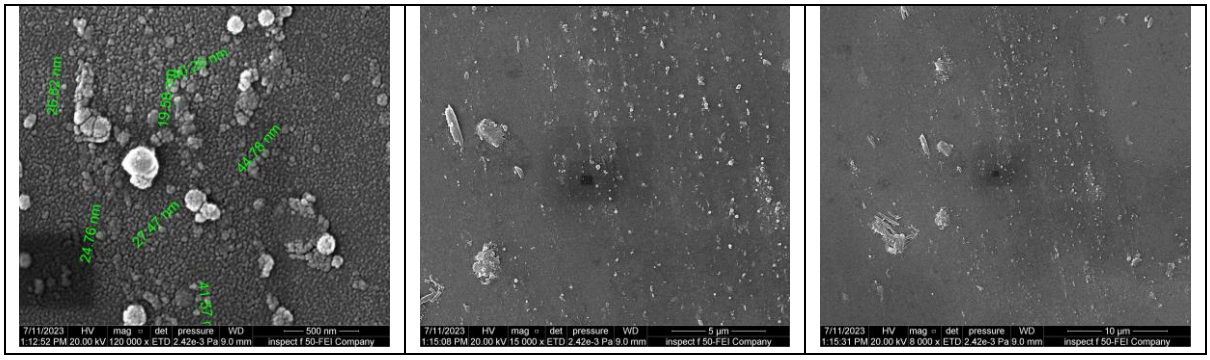

Fig.6: FESEM of Magnetic biochar activation before treatment**.**

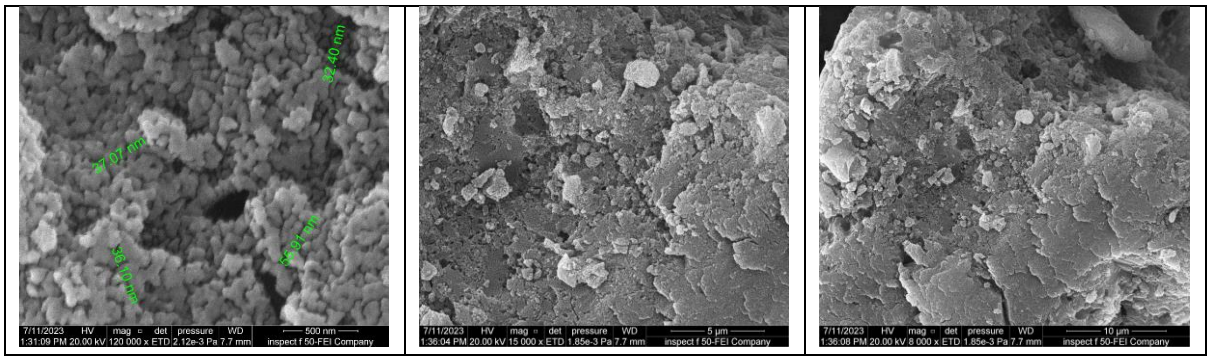

Fig.7: FESEM of cadmium ions (10 ppm) treated by 0.1 gm biochar after 40 minutes

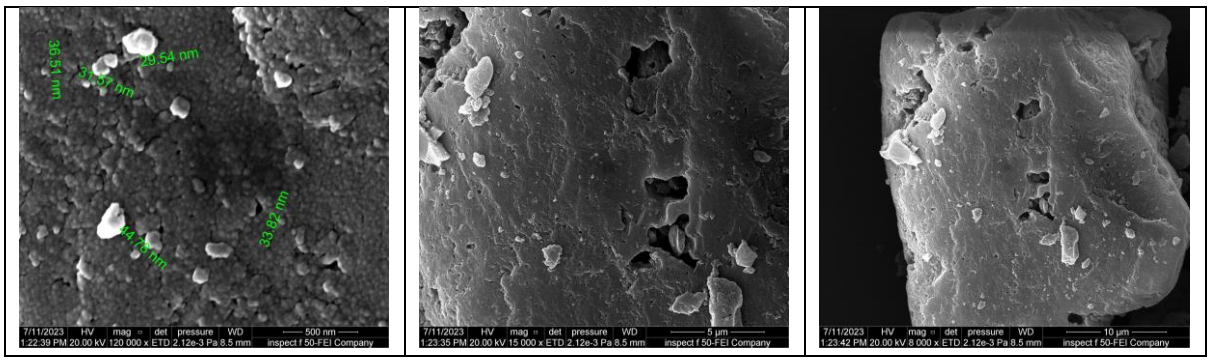

Fig.8: FESEM of cadmium (10 ppm) treated by 0.1 gm magnetic biochar(MBC) after 40 minutes.

The EDX mapping and analysis are used to figure out the basic elements that make up the compound. Furthermore, the EDX technique could give the percentage of

the element in the compound, so the users could determine the type of elements present and the percentage concentration of each element within the sample. Figure (9), is an EDX mapping and analysis of the elements of activated biochar (BC) (0.1 g) treated with cadmium ions at a concentration of 10 ppm, which shows the proportions of the different elements in the sample: cadmium (0.37%), carbon (90.56%), and oxygen (9.7%). While Figure (10), shows EDX mapping and analysis for the elements of magnetic biochar (MBC) (0.1 g) treated with cadmium ions at a concentration of (10) ppm, which shows the proportions of the different elements, cadmium (0.29%), carbon (82.89%), oxygen (15.3%), and Iron (1.53%),

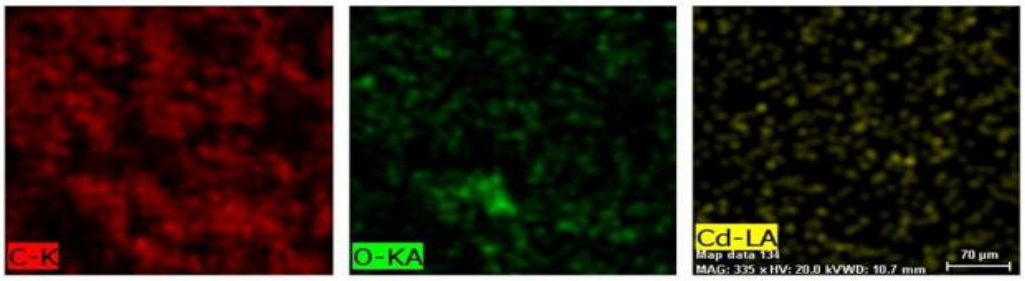

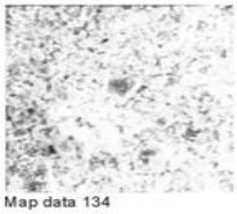

Spectrum: Acquisition

Element	Series	unn. C [wt.%]	norm. C [wt.%]	Atom. C [at.%]	Error (1 Sigma) [wt.%]
Cadmium	L-series	0.37	0.37	0.04	0.06
Carbon	K-series	90.56	90.56	92.97	14.83
Oxygen	K-series	9.07	9.07	6.99	2.55
	Total:	100.00	100.00	100.00	

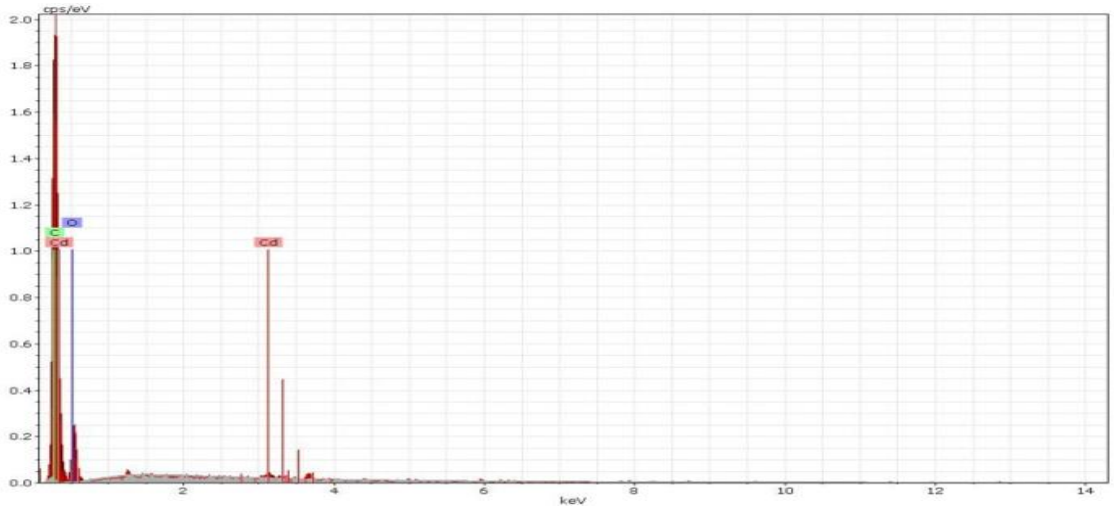

Fig.9: EDX mapping and analysis of 0.1 gm biochar treated with Cd^{2+} at 10 ppm at 40 min.

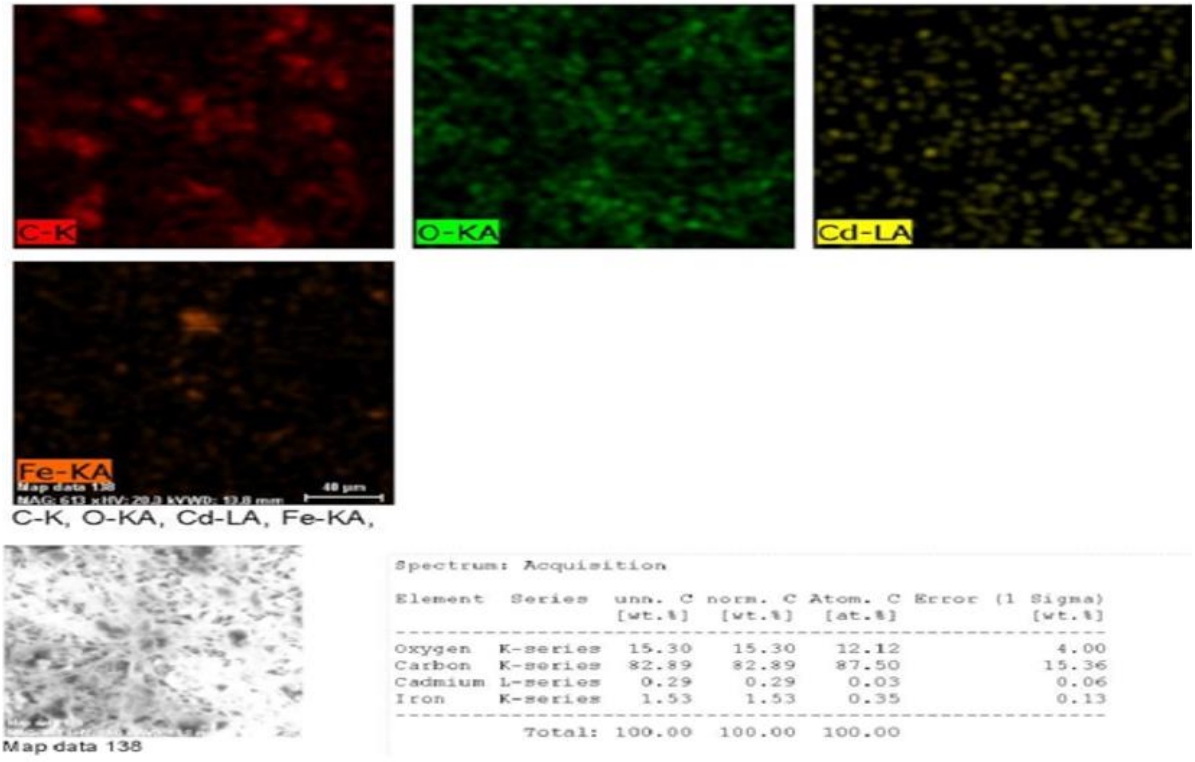

Fig.10: EDX mapping and analysis of 0.1 gm MBC treated with Cd^{2+} at 10 ppm at 40 min.

XRD:

X-ray diffraction (XRD) is another technique to give more information about the structure of activated and magnetic biochar. Figure 11a is an XRD of activated and magnetic biochar. It shows peaks in the disordered carbon crystal plane of biochar activate (Cao *et al.*, 2012; Meng *et al.*, 2015). In addition, the peaks of iron oxide (magnetic nanoparticles) in magnetic biochar are at 30°, 35°, 43°,53°, 57°, and 62.4°, respectively (JCPDS No. 33-0664) (Ruan *et al.*, 2015; Meng *et al.*, 2015). Figure 11b shows biochar activated and biochar activated after treatment with cadmium ions, which find extra low-intensity diffraction peaks at 54° and 73°of Cd-O (GCPDS No. 29-0713). Also, figure 11c shows magnetic biochar and magnetic biochar after treatment with cadmium ions to have extra low-intensity diffraction peaks at 54° and 73°, Cd-O (Yang *et al.*, 2018).

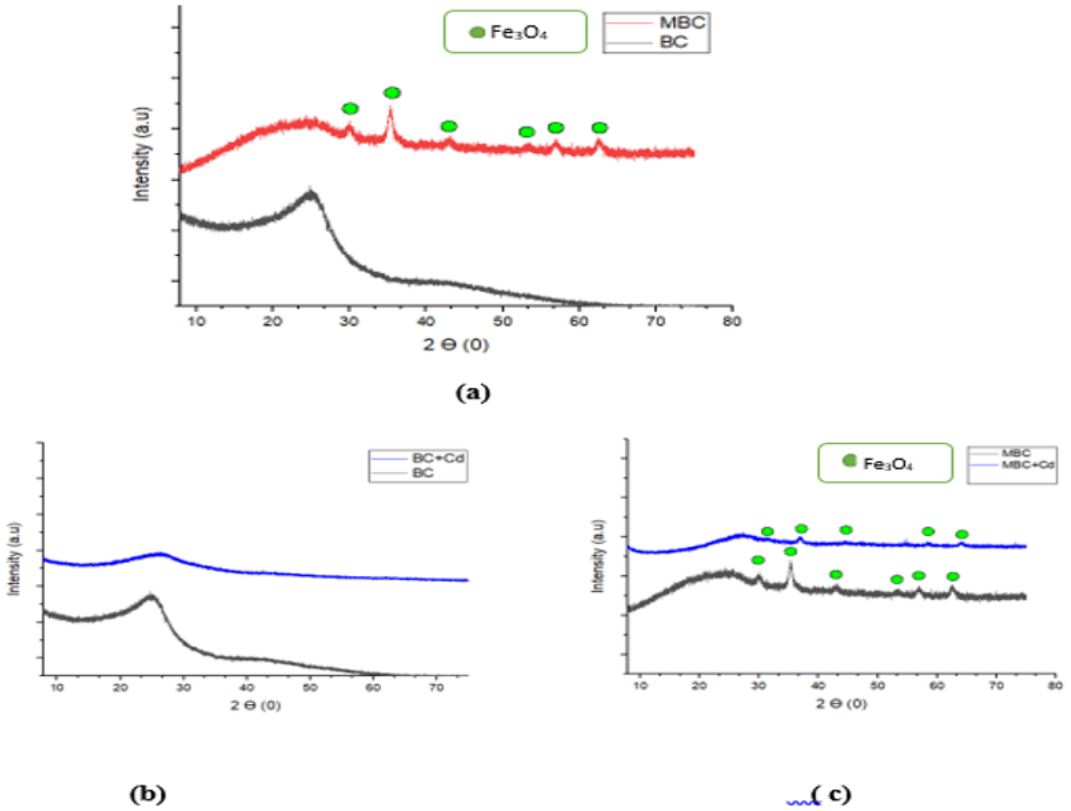

Fig.11: (a) XRD patterns BC and MBC, (b) BC+Cd^{2+}, (c) MBC+Cd^{2+} at 10ppm with 0.1 g of biochar activate or magnetic biochar.

FTIR:

Fourier Transform Infrared spectroscopy (FTIR) is an important technique to determine the new function groups as a new structure in comparison with the structure before the reaction. Figure 12 is biochar before activation, which shows peaks at 3479 cm^{-1}, 3415 cm^{-1} stretching, and 1066 cm^{-1} for O-H bending in the water, 3238 cm^{-1} for C-H stretching, 1622 cm^{-1} for C=C stretching, and 1442 cm^{-1} for C-C stretching in the aromatic ring. However, the biochar after pressing with hydrogen peroxide could activate functional groups such as hydroxyl and carboxyl on the surface. Thus, FTIR gives new peaks of 3370 cm^{-1} for O-H stretching and 1386 cm^{-1} for O-H bending of hydroxyl groups on the surface as phenol. Also, the broad peak from 3200–2600 cm^{-1} for COOH stretching and 1055cm^{-1} bending for C-O-H in carboxyl groups, figure 13, Moreover, the peaks at 1622 cm^{-1} for C=C stretching and 1442 cm^{-1} for C-C stretching in the aromatic ring have shifted to 1597 cm^{-1} and 1412 cm^{-1} respectively, because the conjugated groups of the aromatic ring overlap with new groups (Hurd, 1964; Sun et al.,2023). After the treatment with Cd^{2+} we found a reduction in the intensity of peaks 3371 cm^{-1} and 3199 cm^{-1}, as well as a shifting of the bending peak from 1386 cm^{-1} to 1367 cm^{-1} for O-H of hydroxyl (phenol) because of the coordination bond with cadmium ions (Fig. 14). Not that all, the peak at 1055 cm^{-1} disappeared, and we see peaks at 2955 cm^{-1} and 2922cm^{-1} for coordination carboxyl groups with cadmium ions, which is attributed to the Cd-O of Cd^{2+} (Saha *et al.*, 2007; Guo *et al.*, 2019). Figure 15 is magnetic biochar, which shows a peak at 2958 cm^{-1} and disappears from the bending peak at 1055 cm^{-1} for coordination carboxyl groups with iron oxide (magnetite). The magnetite (Fe-O) stretching modes are represented by the absorption peak at approximately 561 cm^{-1}different peaks corresponding to different organic compounds were also identified (Hwang et al., 2014; Abderrahim *et al.*, 2015;

Taha *et al.*,2022; Jozanikohan and Abarghooei, 2022). Furthermore, the peaks at 1597 cm^{-1} and 1412 cm^{-1} in biochar activate (Fig. 13) shifted to around the normal locations of 1605 cm^{-1} and 1440 cm^{-1} because it is not more conjugated with new functions groups (hydroxyl and carboxyl) after these are coordinated with magnetite. Because make coordination bond with cadmium ions is shown in Figure 14 we see peaks at 2953 cm^{-1} and 2922 cm^{-1} for coordination carboxyl groups, which are attributed to the Cd-O of Cd^{2+}. Also, we found a reduction in the intensity of peaks 3371 cm^{-1} and a shifting of the stretching peak to 3199 cm^{-1} for O-H of hydroxyl (phenol) (Fig.16), because of the coordination bond with cadmium ions (Fourest *et al.,* 1994; Puranik *et al.*, 1999, Forsberg, 1988). According to earlier research, hydroxyl groups have a strong affinity for divalent cations. These hydroxyl and carboxyl groups, which are particularly abundant in biochar, can take on a negative charge and significantly aid in the adsorption of metals.

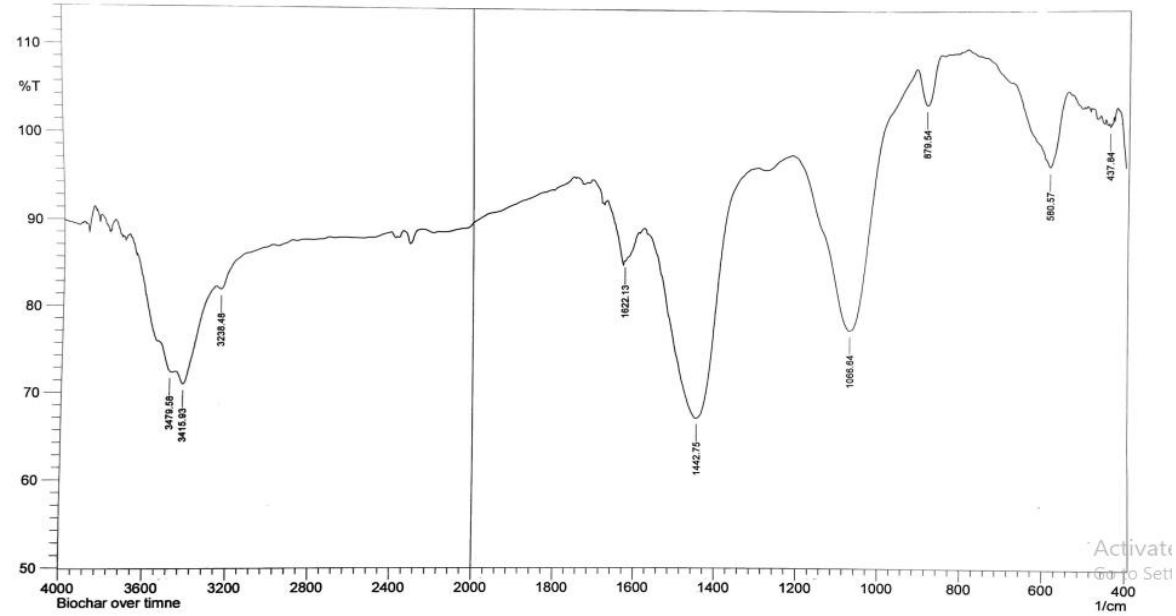

Fig. 12: FT-IR spectrum of biochar *Spirulina platensis* (BC)

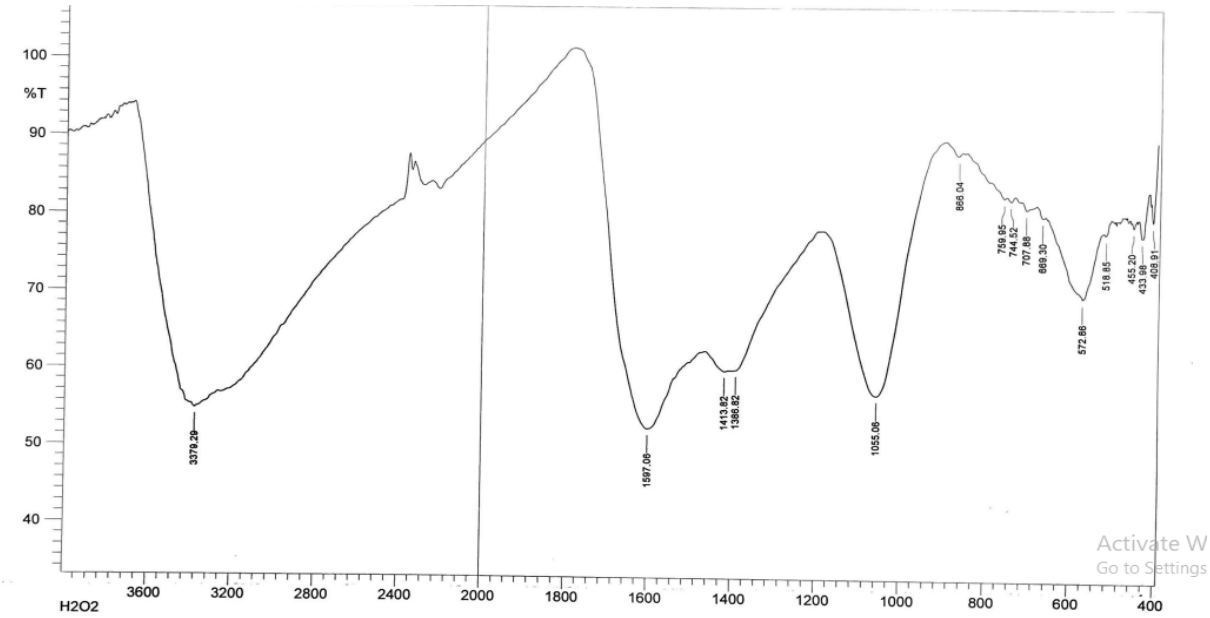

Fig. 13: FTIR spectrum of biochar activate (BC activate)

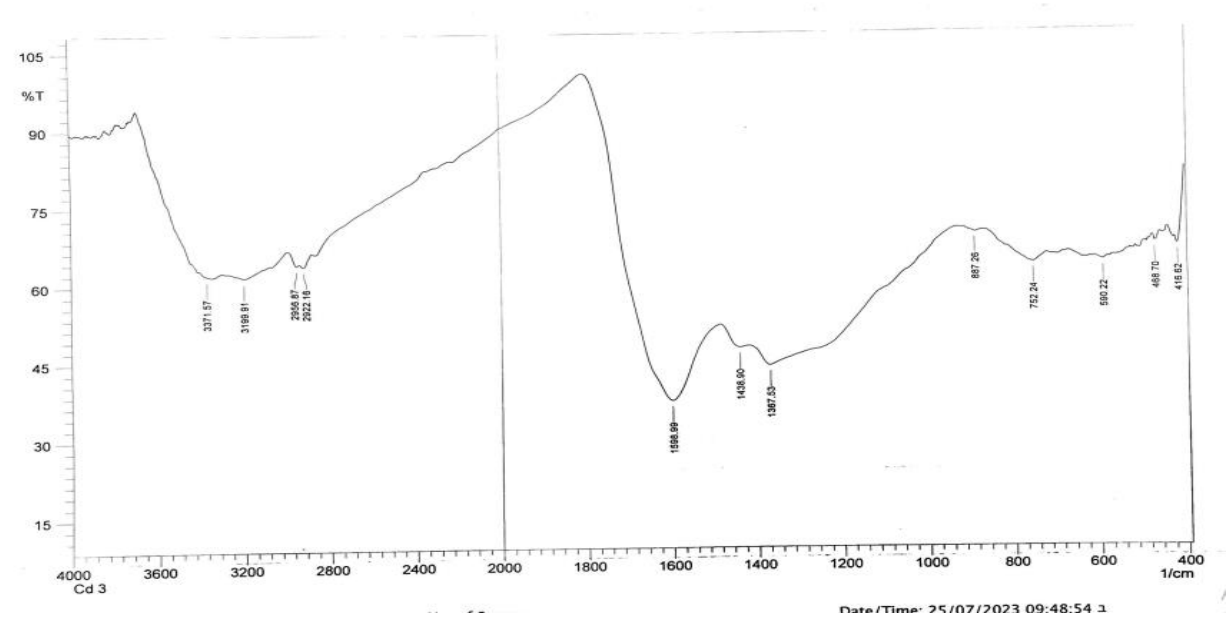

Fig.14: FTIR spectrum of BC activate 0.5 gm treated with Cadmium ions at 10 ppm

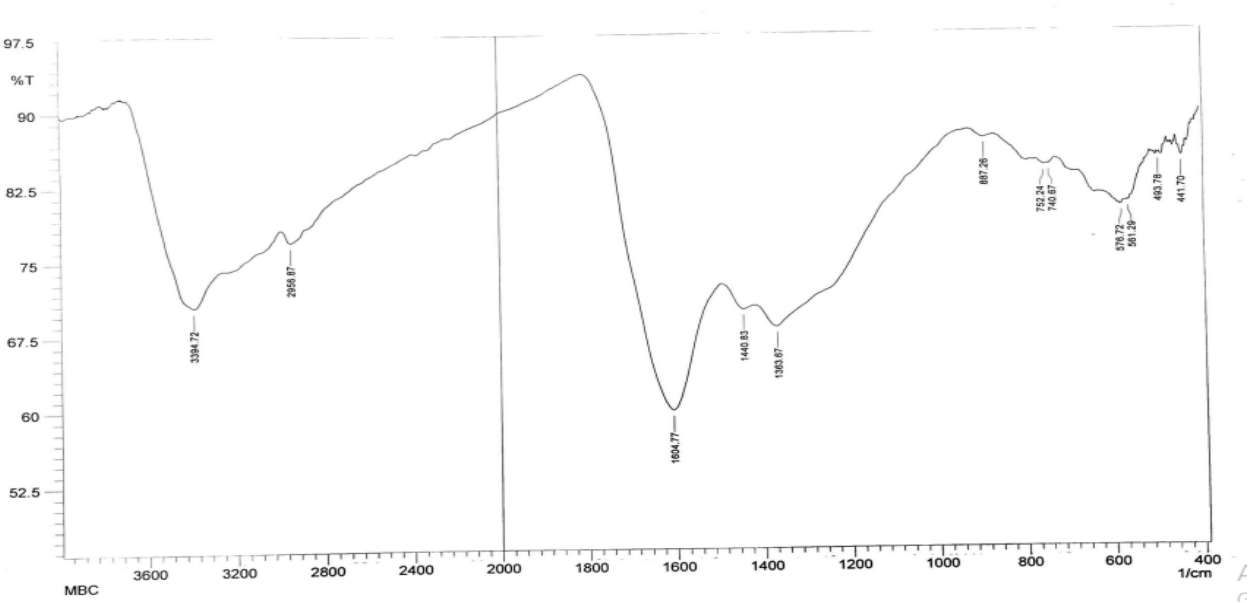

Fig. 15: FTIR spectrum of magnetic biochar (MBC)

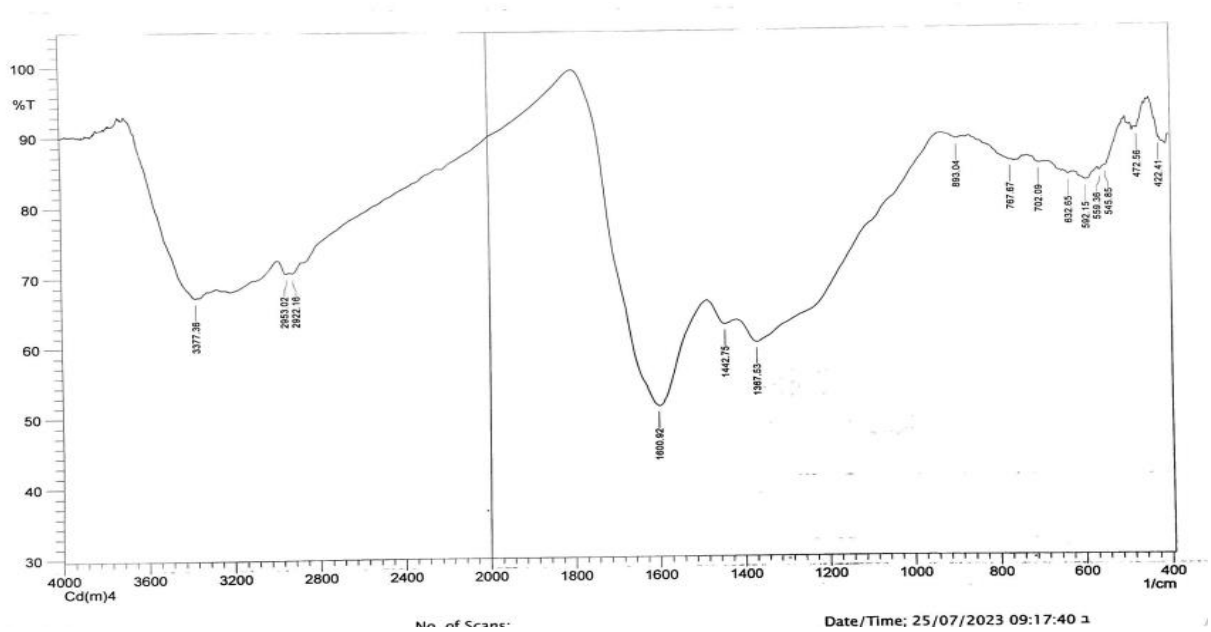

Fig.16: FTIR spectrum of MBC 0.5 gm treated with Cadmium ions at 10 ppm

Conclusion

The adsorption of Cd^{2+} on biochar made from *Spirulina platensis* was shown to be dependent on a number of variables, including biomass dosage, contact time, and the initial concentration of Cd^{2+}. The best conditions for the algal biomass to remove cadmium ions were 0.5 g of biochar activate and MBC at 40 min of contact time, and initial cadmium concentrations of 10 ppm. The potential for removing cadmium ions from aqueous solutions with S. platensis biochar is enormous.

Acknowledgment:

The authors are extremely grateful to Dr. Ahmed Hussein Al-antaki, assistant professor in the chemistry department, the University of Kufa, for continuous cooperation and encouragement.

REFERENCES

Abderrahim, B., Abderrahman, E., Mohamed, A., Fatima, T., Abdesselam, T., & Krim, O. (2015). Kinetic thermal degradation of cellulose, polybutylene succinate and a green composite: comparative study. *World Journal of Environmental Engineering*, *3*(4), 95-110.

AL-Kazazz, F.F., AL-Hakeim, H. k. and AL-Aobaid, H. K., (2016). "study the Interaction Between LH, FSH, and TSH with New synthesized Magnetite Nanoparticles Coated with Dextran" *Medical Journal of Babylon*, Vol. 132, PP. 421-434.

Aniagor, C. O., Elshkankery, M., Fletcher, A. J., Morsy, O. M., Abdel-Halim, E. S., & Hashem, A. (2021). Equilibrium and kinetic modelling of aqueous cadmium ion and activated carbon adsorption system. *Water Conservation Science and Engineering*, *6*(2), 95-104

Baltrėnaitė E, Baltrėnas P, Bhatnagar A, Vilppo T, Selenius M,Koistinen A, Dahl M, Penttinen O (2017) A multicomponent approach to using waste-derived biochar in biofiltration: a case study based on dissimilar types of waste. *International Biodeterioration & Biodegradation*,119:565–576

Cao, Y., Xiao, L., Sushko, M. L., Wang, W., Schwenzer, B., Xiao, J., ... & Liu, J. (2012). Sodium ion insertion in hollow carbon nanowires for battery applications. *Nano letters*, *12*(7), 3783-3787

Forsberg, A., Soderhund, S., Frank, A., Petersson, LR. and Pedersen, M. 1988. Studies on Metal Content in the Brown Seaweed, Fucus vesiculosus,

from the Archipelago of Stockholm. *Environmental Pollution*, 49:245–63.

Fourest, E., Canal, C. and Roux, J.C. 1994. Improvement of heavy metal biosorption by mycelial dead biomasses (Rhizopus arrhizus, Mucor miehei and Penicillium chrysogenum): pH control and cationic activation. *FEMS Microbiology Reviews*, 14:325–32.

Goh, P. S., Lau, W. J., Ismail, A. F., Samawati, Z., Liang, Y. Y., & Kanakaraju, D. (2022). Microalgae-enabled wastewater treatment: A sustainable strategy for bioremediation of pesticides. *Water*, *15*(1), 70

Goswami, R. K., Agrawal, K., Shah, M. P., & Verma, P. (2022). Bioremediation of heavy metals from wastewater: a current perspective on microalgae-based future. *Letters in Applied Microbiology*, *75*(4), 701-717

Guo, X. Z., Chen, S. S., Li, W. D., Han, S. S., Deng, F., Qiao, R., & Zhao, Y. (2019). Series of cadmium (II) coordination polymers based on a versatile multi-N-donor tecton or mixed carboxylate ligands: synthesis, structure, and selectively sensing property. *ACS omega*, *4*(7), 11540-11553

Hassan, P. B., Rasheed, R. O., & Zargoosh, K. (2022). Cadmium and Lead Removal from Aqueous Solution Using Magnetite Nanoparticles Biofabricated from Portulaca Oleracea Leaf Extract. *Journal of Nanomaterials*, Volume 2022 | Artic le ID 1024554 | https://doi.org/ 10. 1155/2022/1024554

Hurd, C. D. (1964). Basic Principles of Organic Chemistry. John D. Roberts and Marjorie C. Caserio. Benjamin, New York, 1964. xxvi+ 1315 pp. Illus. $13.90. *Science*, *146*(3646), 911-911

Hwang, S. W., Umar, A., Dar, G. N., Kim, S. H., & Badran, R. I. (2014). Synthesis and characterization of iron oxide nanoparticles for phenyl hydrazine sensor applications. *Sensor Letters*, *12*(1), 97-101.

Jasim, A. M., & Alzurfi, S. K. L. (2022). Compared cadmium adsorption from biochar and magnetite biochar in water.*International Journal of Health Sciences*,6(S5), 11603–11621.

Jozanikohan, G., & Abarghooei, M. N. (2022). The Fourier transform infrared spectroscopy (FTIR) analysis for the clay mineralogy studies in a clastic reservoir. *Journal of Petroleum Exploration and Production Technology*, 1-14.

Kadhum, A. T., & Albayati, T. M. (2022). Desulfurization of real diesel fuel onto mesoporous silica MCM-41 implementing batch adsorption process: Equilibrium, kinetics, and thermodynamic studies. *Engineering and Technology Journal*, *40*(09), 1144-1157

Kim, S., Park, C. M., Jang, A., Jang, M., Hernández-Maldonado, A. J., Yu, M., ... & Yoon, Y. (2019). Removal of selected pharmaceuticals in an ultrafiltration-activated biochar hybrid system. *Journal of Membrane Science*, *570*, 77-84.

Lei, T., Li, S. J., Jiang, F., Ren, Z. X., Wang, L. L., Yang, X. J., ... & Wang, S. X. (2019). Adsorption of cadmium ions from an aqueous solution on a highly stable dopamine-modified magnetic nano-adsorbent. *Nanoscale Research Letters*, *14*, 1-17

Luo, M.; Lin, H.; Li, B.; Dong, Y.; He, Y.; Wang, L**. 2018,** A novel modification of lignin on corncob-based biochar to enhance removal of cadmium from water. *Bioresource Technology, 259*, 312–318.

Meng, X., Savage, P. E., & Deng, D. (2015). Trash to treasure: from harmful algal blooms to high-performance electrodes for sodium-ion batteries. *Environmental Science & Technology*, *49*(20), 12543-12550

Pragya, N., Pandey, K. K., & Sahoo, P. K. (2013). A review on harvesting, oil extraction and biofuels production technologies from microalgae. *Renewable and sustainable energy reviews*, *24*, 159-171.

Priatni, S., Ratnaningrum, D., Warya, S., & Audina, E. (2018, June). Phycobiliproteins production and heavy metals reduction ability of Porphyridium sp. In *IOP Conference Series: Earth and Environmental Science* (Vol. 160, No. 1, p. 012006). IOP Publishing

Puranik, P.R., Modak, J.M. and Paknikar, K.M. 1999. A comparative study of the mass transfer kinetics of metal biosorption by microbial biomass. *Hydrometallurgy*, 52:189.

Qiu M, Liu L, Ling Q, Cai Y, Yu S, Wang S, Fu D, Hu B, Wang X (2022) Biochar for the removal of contaminants from soil and water: a review. *Biochar journal*, 4:19

Ruan, Z. H., Wu, J. H., Huang, J. F., Lin, Z. T., Li, Y. F., Liu, Y. L., ... & Jiang, G. B. (2015). Facile preparation of rosin-based biochar coated bentonite for supporting α-Fe 2 O 3 nanoparticles and its application for Cr (VI) adsorption. *Journal of Materials Chemistry A*, *3*(8), 4595-4603.

Saha, B., Das, S., & Chattopadhyay, K. K. (2007). Electrical and optical properties of Al doped cadmium oxide thin films deposited by radio frequency magnetron sputtering. *Solar energy materials and solar cells*, *91*(18), 1692-1697.

Sun, F., Tan, S., Cao, H. J., Lu, C. S., Tu, D., Poater, J., ... & Yan, H. (2023). Facile Construction of New Hybrid Conjugation via Boron Cage Extension. *Journal of the American Chemical Society*, *145*(6), 3577-3587

Taha, A. B., Essa, M. S., & Chiad, B. T. (2022). Spectroscopic Study of Iron Oxide Nanoparticles Synthesized Via Hydrothermal Method. *Chemical Methodologies*, *6*(12), 977-984

Wang, Y. X., Gupta, K., Li, J. R., Yuan, B., Yang, J. C. E., & Fu, M. L. (2018). Novel chalcogenide based magnetic adsorbent KMS-1/L-Cystein/Fe3O4 for the facile removal of ciprofloxacin from aqueous solution. *Colloids and Surfaces A: Physicochemical and Engineering Aspects*, *538*, 378-386

Yang, F., Zhang, S., Li, H., Li, S., Cheng, K., Li, J. S., & Tsang, D. C. (2018). Corn straw-derived biochar impregnated with α-FeOOH nanorods for highly effective copper removal. *Chemical Engineering Journal*, *348*, 191-201.

Yusuff, A. S. (2022). Adsorptive removal of lead and cadmium ions from aqueous solutions by aluminium oxide modified onion skin wastes: Adsorbent characterization, equilibrium modelling and kinetic studies. *Energy & Environment*, *33*(1), 152-169